Solvent Effects on Solute Electronic Structure and Properties: Theoretical Study of a Betaine Dye Molecule in Polar Solvents

Tateki Ishida and Peter J. Rossky*

Institute for Theoretical Chemistry, Department of Chemistry and Biochemistry, University of Texas at Austin, Austin, Texas 78712

Received: November 8, 2000

The electronic structure of the betaine dye molecule, pyridinium- *N*-phenoxide [4-(1-pyridinio)phenolate] including the effects of geometry and polar solvents, has been studied at an ab initio level using the reference interaction site model self-consistent-field (RISM-SCF) method. Acetonitrile (CH_3CN) and water (H_2O) were selected as polar solvents. We obtain both the optimized solute geometry in solution and the total free energy profile with respect to variation in the torsion angle between the pyridinium and phenoxide rings and analyze the various electronic and solvation contributions. The betaine molecule in the gas phase has a twisted geometry, which is slightly more twisted in solution. In acetonitrile, the calculated structure shows good agreement with earlier semiempirical results for the minimum free energy structure. It is shown that the solute dipole moment is strongly enhanced in polar solution, also in accord with earlier semiempirical calculations. However, in solution, there is relatively little change in dipole moment with changes in the torsion angle, in contrast to the marked variation in the gas phase. Correspondingly, the solvation free energy is only weakly more negative with increasing twist. Electron correlation in the solute molecule is shown to play an important role in the torsional free energy, destabilizing the twisted form. This destabilization decreases by a factor of 4 from the gas phase to water, with increasing charge localization induced by the solvent. The implications of these results for interaction site models of charge-separated conjugated molecules in solution are discussed.

I. Introduction

Solvent effects on solute structure and their spectroscopic signature are important themes for solution chemistry. The solute−solvent interaction can be important in determining structural stability and can also influence the electronic structure directly. Among readily observed effects, solvent-induced effects on the electronic absorption spectrum are especially well-known and are referred to as solvatochromism.[1,2] Since the solvatochromic shift depends on solvent polarity, it has been used as a measure of solvent character. A number of scales for solvent properties have been defined and used as empirical solvation parameters.[1,3] To obtain these parameters, it is necessary to choose probe molecules that are particularly sensitive to solvent polarities. That is, solvatochromic shifts report the effects of the solvent on the electronic energy and electronic structure of the solute molecule. A better understanding of solvatochromism provides one strong motivation to study the details of the solute molecule.

Betaine-30 (Reichardt's dye)[1] has often been chosen as the probe solute molecule. Betaine-30 is very sensitive to solvent polarities, and it is known that in water the peak of the absorption band for betaine-30 is blue shifted[1] by over 20 000 cm^{-1} compared to nonpolar media. This occurs because the electronic structure has a charge-separated character in the ground state, and the dipole moment is reduced in the excited state due to charge transfer after the excitation.[4,5] On the basis of this, it is clear that the electronic structure of the solute molecule is a key element in fully understanding such spectral features.

At the same time, the charge-transfer character of this excitation has been exploited as a probe of intramolecular electron transfer. Spectral characteristics have been used to investigate molecular reorganization.[4,6,7] Back electron transfer in photoexcited systems has been the subject of both experimental ultrafast spectroscopic studies[4] and a number of theoretical dynamics studies.[5,8−12]

To accurately interpret the experiments on this complex system requires an understanding not only of the electronic energy surfaces of the isolated molecule but also an understanding of the coupled interaction of solvent and solute, including the perturbation of the electronic structure of the solute by the polar solvent. A semiempirical quantum chemical study of betaine-30 in acetonitrile[13] has suggested that such interaction not only affects the spectral maximum but also substantially impacts solute conformational contributions to the line shape. The local solute−solvent interactions, such as hydrogen bonding, can play an important role in determining the solvent distribution around a solute[14] implying that a molecular-level solvent treatment may be critical.

To investigate these effects, a method must be applied that takes into account both the solute electronic structure and the solvent effects in a consistent manner. Several studies of betaine systems that include both the solute electronic structure and solvent effects have been carried out. Zerner and co-workers[15] carried out semiempirical calculations of betaine-30, in which solvent effects on the electronic spectrum were treated with a continuum solvent self-consistent reaction field (SCRF) method. However, in their study, the important central torsion angle between the pyridinium and the phenoxide ring was not discussed. This angle is important since the excitation of primary importance is in the π-electron system. Bartkowiak and Lipiński[16] used a semiempirical method and the Langevin dipoles/Monte Carlo method for solvents, and reported that the central

10.1021/jp0041104 CCC: $20.00
Published on Web 01/03/2001

angle became about 90° in aqueous solution. In these studies, the solvent molecular configurations were not treated explicitly. Lobaugh and Rossky[13] performed molecular dynamics simulations in acetonitrile combined with the Pariser−Pople−Parr semiempirical electronic structure theory, and found that the equilibrium central torsion angle was only partially twisted at 53°. Mente and Maroncelli[17] have obtained 48° for this angle, in the gas phase, which is close to the result of Lobaugh and Rossky. For *p*-bromo substituted betaine-30, crystallography yields 65° for this angle.[18]

An unusually large electronic polarization of the solute by the solvent has also been noted. In SCRF treatments, increases of dipole moment from 13 D in the gas phase to 19 D in acetonitrile have been reported.[15] In the molecular simulations in acetonitrile,[13] a similar increase from 15.8 to 24.95 D was obtained. Since treatments of solvatochromism and solvation dynamics are often based on fixed charge interaction site models,[17,19,20] the large changes in electronic distribution reflected by the dipole moment would need to be reflected in such models. Hence, a further exploration of electronic polarization, including validation of these large changes, is required.

In a molecule such as betaine-30, there are two delocalized ring systems: the heteroaromatic pyridinium ring and the phenoxide ring. In such cases, electron correlation between rings can affect the structure of the solute molecule. Thus, the electron correlation energy will change with the relative geometry of the two rings. Further, in general, the response in solution is likely to depend on polarization by the solvent. To consider the electron correlation effects and geometry optimization simultaneously, it is necessary to obtain the electronic structure accurately. Also, a method that treats solvent molecules at a molecular level is desirable. The reference interaction site model self-consistent-field (RISM-SCF) method[21−23] is an ab initio electronic structure theory that takes into account the molecular aspects of the solvent molecules which has provided successful explanations for various problems in solution chemistry.[14,24] In the present research, we employ the RISM-SCF method to address the geometrical and electronic structure of the subject solute molecule in solution.

Although, in the gas phase, many ab initio level theoretical studies have been performed for molecules such as biphenyl[25−28] and 4,4′-bipyridine,[29−31] in which the two ring moieties are the same, few studies of molecules composed of pyridinium and phenoxide rings have been reported.[32,33] In the present study, we consider the simplest betaine, pyridinium-*N*-phenoxide betaine [4-(1-pyridinio)phenolate, see Figure 1] as the solute molecule. We apply the RISM-SCF method to investigate the solute properties, solvation free energy, and the dependence of electron correlation effects on the geometry of the solute molecule in both acetonitrile (CH_3CN) and water (H_2O) solvents, as well as in the gas phase.

This paper is organized as follows. In the following section, we present the theoretical method applied to the target systems, and the details of the calculation procedure are also given. In section III, the results for geometry and electronic structure obtained for the betaine solute in polar solvents are shown. The optimized structure of the solute in solution and the solvation free energy surfaces with respect to the central torsion angle in the solute molecule are reported and discussed, as is the change of the solute dipole moment. The electron correlation energy of the solute molecule in solution and its dependence on solute geometry and solvent is also discussed. Conclusions of this work are summarized in section IV.

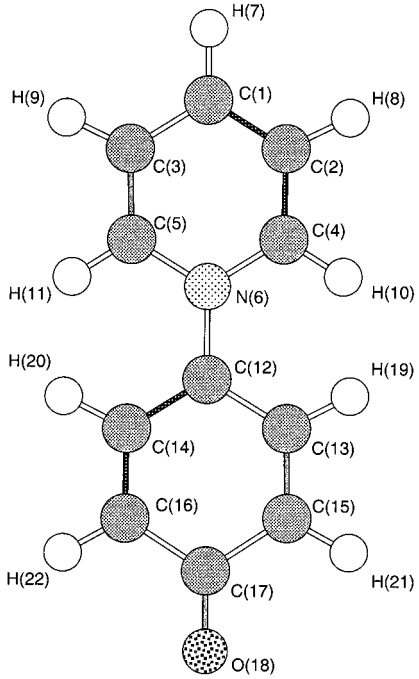

Figure 1. Molecular geometry and site labels for 4-(1-pyridinio)-phenolate.

II. Theoretical Methods

A. RISM-SCF Method. Many papers have previously presented details of the RISM-SCF method.[21−23] Therefore, we only briefly present the theoretical methods employed here.

The solvation free energy of the system is defined in RISM-SCF theory as

$$G = \langle \Psi | \hat{H}_{\mathrm{gas}} + \Delta\hat{\mu}_{\mathrm{sol}} | \Psi \rangle$$

where Ψ is the solute electronic wave function, $\hat{H}_{\mathrm{gas}}$ is the electronic Hamiltonian of the solute molecule in the gas phase, and $\Delta\hat{\mu}_{\mathrm{sol}}$ represents the excess chemical potential due to solvation. The solvation free energy G is a functional with respect to the solute molecular orbitals ϕ_i, which themselves depend on solvent. The excess chemical potential $\Delta\hat{\mu}_{\mathrm{sol}}$ is the functional of the solute−solvent correlation functions $h_{\alpha\gamma}$ (total correlation) and $c_{\alpha\gamma}$ (direct correlation), where α and γ represent sites on solute and solvent molecules, respectively.

The solvated Fock operator underlying the molecular orbitals in solution is constructed from the Fock operator for the gas phase $\hat{F}_{gas}$ and the electrostatic potential originating in the solvent around the solute

$$V_\alpha = \rho \sum_\gamma q_\gamma \int \frac{g_{\alpha\gamma}(r)}{r} \mathrm{d}\mathbf{r} \qquad (2)$$

where ρ and q_γ represent the solvent(v) density and the partial charge on the solvent site γ, respectively, and $g_{\alpha\gamma}(r) = h_{\alpha\gamma} + 1$ is the radial distribution function between the solute site α and the solvent site γ. Also, the solute (u) excess chemical potential is given by

$$\Delta\mu_u = \frac{\rho}{2\beta} \sum_{\alpha\in u} \sum_{\gamma\in v} \int_0^\infty 4\pi r^2 \mathrm{d}r (h_{\alpha\gamma}^2 - 2c_{\alpha\gamma} - h_{\alpha\gamma}c_{\alpha\gamma}) \qquad (3)$$

where $\beta = 1/k_{\mathrm{B}}T$ (k_{B} is the Boltzmann constant). The correlation functions $h_{\alpha\gamma}$ and $c_{\alpha\gamma}$ are obtained by solving the XRISM

equations[34−36] which incorporate the hypernetted-chain (HNC) closure relation.

With the orbital energies obtained via the *solvated* Fock operator, the correlation energy of the solute molecule in solution is evaluated here by employing the Møller−Plesset second-order perturbation method[24,37]

$$E_{\mathrm{MP2}}^{\mathrm{sol}} = \frac{1}{4}\sum_{abrs}\frac{|\langle ab||rs\rangle|^2}{\epsilon_a + \epsilon_b - \epsilon_r - \epsilon_s} \tag{4}$$

where ϵ_a and ϵ_b are the occupied orbital energies, and ϵ_r and ϵ_s the unoccupied. $\langle ab||rs\rangle$ indicates the anti-symmetrized two-electron integral.

B. Computational Details. In both the gas and solution phases, all of the ab initio calculations were carried out at the restricted Hartree−Fock (RHF) level, with the (9s5p1d/4s1p)/[3s2p1d/2s1p] basis set, which possesses valence double-ζ plus polarization (DZP) quality.[38] Throughout all optimizations, both the pyridinium and the phenoxide ring were constrained to be planar with C_2 symmetry. To estimate the electron correlation energy in the gas phase, the optimized geometry from the RHF level was used. The MP2 calculations were performed with the RHF level optimized structures. In addition, we have also carried out geometry optimization for the ground state in the gas-phase including electron correlation using the Complete Active Space (CAS)SCF method. The active space used in the CASSCF geometry optimization included 11 active spaces (12 electrons), which is constructed from π and π^* orbitals for the pyridinium and phenoxide ring moieties, respectively, 6π-valence active orbitals, and the *n* (nonbonding) orbital on the oxygen. Both RHF and MP2 calculation were also carried out for the biphenyl molecule to compare the characteristic properties with that of the betaine system.

In solution, the analytical energy gradient technique was applied for optimization of the solute geometry.[23] The partial charges on the solute atomic sites were determined by least-squares-fitting to the electrostatic potential, which was evaluated at a number of grid points, about 4200 points, around the solute. We note that this number of points is relatively large compared to typical implementations. However, the symptom of using too few points is the appearance of nonsystematic "noise" in charges, electronic energies, and solvation free energies with changes in solute geometry. In the present case, where it will be seen that solute charge distribution varies considerably with the geometric changes of interest, this is a particular issue. There remain very small nonsystematic variations in the data shown in the figures which can be traced to this origin, but are not of sufficient magnitude to warrant further refinement. We also note that, recently, three-dimensional RISM-SCF calculations (3D-RISM-SCF) without radial averaging have been reported.[39] In that paper,[39] it was found that computed solute dipole moments in aqueous solution are enhanced both in the original RISM-SCF and in the 3D-RISM-SCF, and, further, that the results from the original method are comparable to those by the 3D-RISM-SCF model. Therefore, our application of the considerably simpler original RISM-SCF to the present study is justified. For estimates of correlation energy effects in each solvent, the calculations were executed with the optimized geometry from the RISM-SCF method at each point, using the RISM-SCF wave function as the reference state.

For the RISM calculation, all the parameters for both the solute and solvent molecule are adopted from standard sets used in computer simulation.[40−42] These are summarized in Table 1. The Simple Point Charge (SPC)[43]-like model was employed as a model of water solvent; SPC is supplemented by Lennard-Jones parameters for the H atom (σ = 1.0 Å and ϵ = 0.056 kcal·mol^{-1}). All calculations were carried out under the condition T = 298.15 K.

TABLE 1: Parameters for Solvents and Solute

solvent[a]	site	q/e	σ/Å	ϵ/kcalmol^{-1}
H_2O	H	0.41	1.000	0.056
	O	−0.82	3.166	0.155
CH_3CN	CH_3	0.15	3.775	0.206
	C	0.28	3.650	0.150
	N	−0.43	3.200	0.169

solute[b]	σ/Å	ϵ/kcalmol^{-1}
C	3.550	0.070
O	2.960	0.210
N	3.250	0.170
H	2.420	0.030

[a] Data from ref 43 for H_2O, ref 42 for CH_3CN. [b] References 40 and 41.

TABLE 2: Selected Optimized Geometric Parameters in the Gas Phase and Solution at the SCF Level

	gas phase[a]	in CH_3CN	in H_2O
	Bond Length		
r(C(1)−C(2))	1.388 (1.387)	1.387	1.389
r(C(2)−C(4))	1.377 (1.383)	1.375	1.373
r(C(4)−N(6))	1.346 (1.345)	1.340	1.341
r(C(12)−N(6))	1.429 (1.424)	1.447	1.448
r(C(17)−O(18))	1.222 (1.228)	1.245	1.308
	Bending Angle		
C(4)−N(6)−C(5)	118.76 (118.71)	119.76	120.48
C(13)−C(12)−C(14)	118.84 (118.96)	119.20	120.04
	Torsion Angle		
C(5)−N(6)−C(12)−C(13)	39.91 (40.72)	45.56	46.79

[a] Values in parentheses are from optimized CASSCF calculation.

III. Results and Discussion

A. Solute Geometry. In this section, we discuss the solute geometry in gas and solution phases.

In Table 2, the optimized solute geometric parameters are shown.

1. Gas Phase. The central inter-ring torsion angle χ between N(6) and C(12) (see Figure 1) has an optimum value of 40° at the RHF level. Since the π-electrons are delocalized between fragments, the coplanar conformation is favored by conjugation but, due to the steric repulsion between the hydrogen atoms in each fragment (for example, between H(10) and H(19) in Figure 1), the solute geometry is changed so that the steric hindrance is minimized. Therefore, the twisted form is reasonable for the optimized structure. In previously published results, 25.0° (semiempirical AM1 level)[16,32] and 30.4° (density functional theory (DFT) method)[33] have been reported. Also, for the central C(12)−N(6) bond length between the pyridinium and phenoxide rings, our result of 1.429 Å, calculated with the HF method, is longer than the reported DFT result, 1.406 Å.[33] Optimized CASSCF results (Table 2) suggest the RHF value as more accurate.

In Figure 2, the potential energy curve with respect to the torsion angle in gas phase is shown for alternative methods of calculation. For the RHF level calculation, the minimum appears at about 40°, as noted. Inclusion of the MP2 level correlation energy with the structure optimized at the RHF level leads to somewhat of a change in the potential energy minimum to about 30°, but the energy difference from the RHF result is within

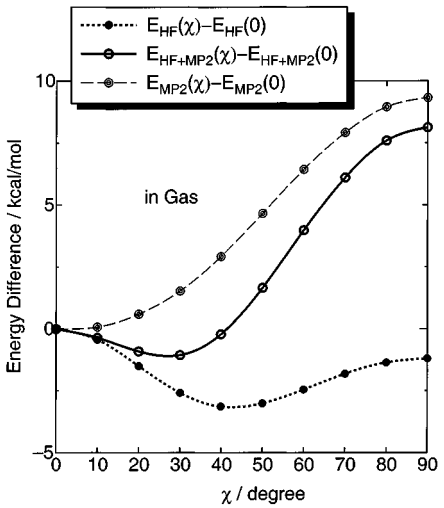

Figure 2. Energy profiles for central torsion angle, relative to $\chi = 0$, in the gas phase. The solute electronic energy E_{HF} and the electronic correlation energy E_{MP2} and the sum are shown.

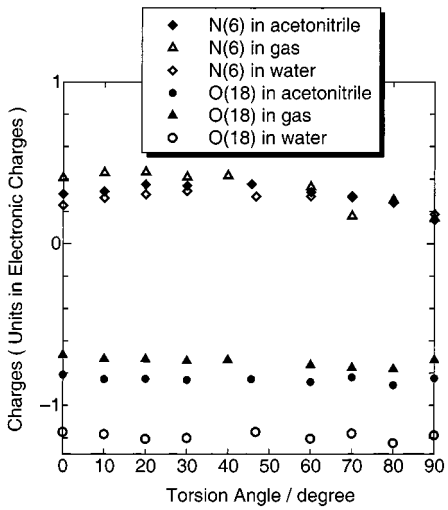

Figure 3. Partial charges on N(6) and O(18) obtained in each solvent as a function of torsion angle.

about 1 kcal/mol. To test the reliability of the RHF description, we carried out CASSCF level calculations with geometry optimization. The results are very close to the RHF value (see Table 2). The small difference in torsion angle between RHF and CASSCF is likely accidental. At the same time, the ~10° difference between the CASSCF and RHF + MP2 torsional minima may be deceptive. The torsional potential is quite flat in this region and the MP2 calculations are not geometry optimized. In fact, calculations at the CASSCF level show that the energy difference (relative to 0°) between the RHF + MP2 energy at its torsional minimum and the corresponding relative difference for CASSCF is only about 0.2 kcal/mol. This is to be compared to the ~3 kcal/mol difference comparing RHF and RHF + MP2. We note here that the relatively strong variation in correlation energy with torsional angle evident in Figure.2 is a characteristic of the large charge separation in the betaine molecule. Calculations carried out for biphenyl show that the effect is much smaller, as discussed below (section C).

Although electron correlation is significant in optimizing the overall solute geometry, in the present study we focus on the qualitative analysis of the geometric changes in solution. On the basis of the comparisons above, hereafter, we will proceed with discussions based on the calculated results and optimized parameters at the RHF level, with MP2 correlations at RHF geometries. In particular, the overall torsional effects appear reasonably well described at this level, as shown in Table 2.

2. In Solution. For the optimized structures, the bending angle, C(4)−N(6)−C(5), in the pyridinium moiety increases slightly and the bond length, r(C(2)−C(4)), is shortened slightly as solvent polarities increase (see Table 2). Consequently, the pyridinium moiety shrinks slightly along the same direction as the central C−N bond. On the other hand, in the phenoxide ring, although the angle C(13)−C(12)-C(14) is increased slightly in polar solvents, the C(13)−C(15) bond stretches and the C(12)−C(13) bond becomes slightly shorter as the solvent media becomes more polar. In addition, the C−O bond length also increases. The central C−N bond lengths are 1.447 and 1.448 Å in acetonitrile and aqueous solution, respectively, which compare with 1.429 Å in the gas phase.

In summary, geometric changes occur in the pyridinium moiety so that the solute molecule becomes more compact, but the phenoxide moiety becomes larger along with the direction of the central bond in solution. The central C−N bond also becomes longer in comparison with that in the gas phase. These geometric changes are associated with electronic polarization and enhanced solute dipole moment, as solvent polarity increases, as discussed below.

B. Solute Partial Charge and Dipole Moment. Among partial charges on the solute sites, we focus on the heteroatoms N(6) and O(18). As shown in Figure 3, the partial charges on the nitrogen atom in the pyridinium ring and the oxygen atom in the phenoxide ring are polarized in water to a greater extent than in acetonitrile. The enhancement of the partial charge on the oxygen site is notably more dependent on solvent polarities. On the other hand, the magnitude of the partial charge on the nitrogen atom is not much affected by solvent polarity. Also, as discussed in the previous section, the pyridinium ring shrinks and the phenoxide ring expands in the central C−N bond direction in polar solvents. Electrons evidently become more localized on the phenoxide ring. This is consistent with the results displayed in Figure 3. Furthermore, it should be noted that the degree of charge localization is far smaller on the nitrogen atom than on the oxygen site, and that the nitrogen charge is far different from the unit charge that one would infer from a simple valence bond structure.

In Figure 4, the corresponding changes of the solute dipole moment in the gas phase, acetonitrile, and aqueous solution are shown with respect to the solute torsion angle. We note that, in the gas phase, the solute dipole moment at the optimized structure estimated from the partial charges, 15.39 D, is completely consistent with that calculated directly from the ab initio wave function (RHF level), 15.43 D. The solute dipole moment becomes notably larger with increasing torsion angle, particularly in the gas phase. Also, as shown in Figure 5 the central C−N bond lengthens in the gas phase as the torsion angle increases. This corresponds to reduction of π-electron conjugation between the two main rings. However, the change in bond length in polar solvents is best described as very small ($\lesssim$0.01 Å). It is also seen in Figure 5 that the value is close to that obtained in the gas phase at 90°. This suggests that the charge localization that is promoted by twisting in the gas phase is largely accomplished by the polarization by solvent in the polar solvents. Results in Figure 4 and below are in accord with this view.

In Figure 6, we show the change of the total charge in each ring with respect to the torsion angle. As evident in this figure, when the torsion angle between the two rings increases in the

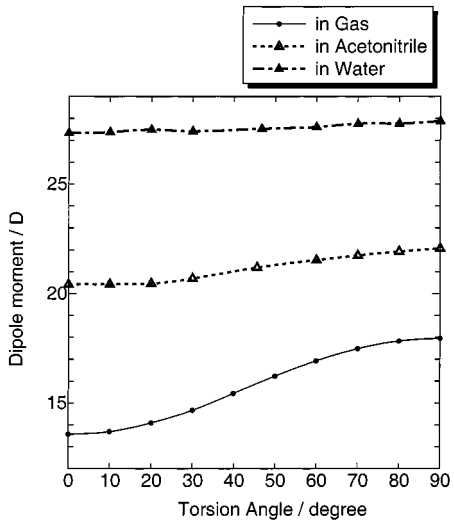

Figure 4. Changes of the solute dipole moment (derived from partial charges) with central torsion angle in the gas phase, acetonitrile, and aqueous solution.

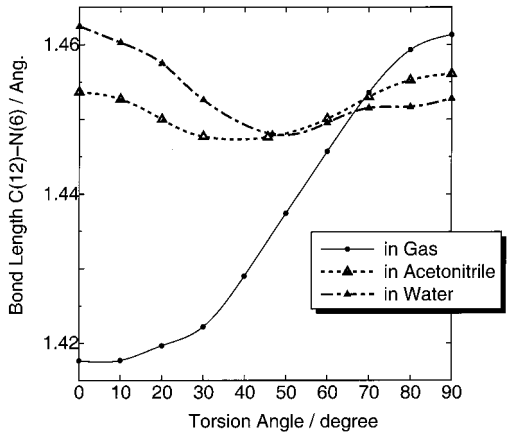

Figure 5. Variations of the central C−N bond length of the solute molecule with central torsion angle for the RHF optimized structure in the gas phase, acetonitrile, and aqueous solution.

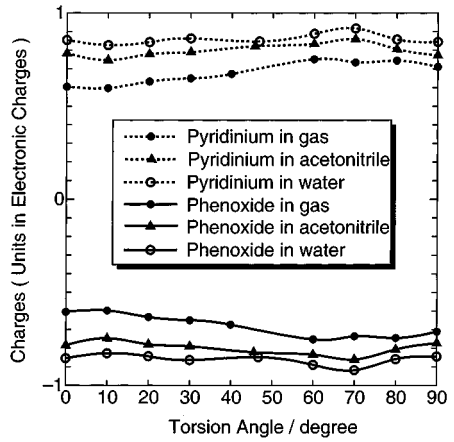

Figure 6. Variation of the net partial charge of the pyridinium and phenoxide rings in the gas phase and solvents, as a function of torsion angle.

gas phase, charge separation is promoted. In the perpendicular conformation, the total charge in the phenoxide ring is more negative by about 0.1 in comparison with that in the coplanar form. These changes correspond to increase of the solute dipole moment in the gas phase (see Figure 4). In polar solvents, the solute dipole moment is also enhanced due to increase of the

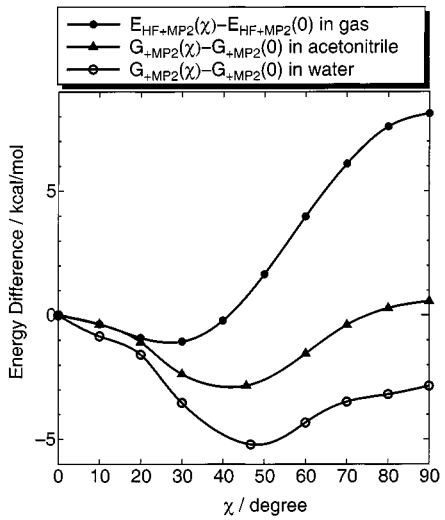

Figure 7. Comparisons of the free energy differences relative to planar geometry in the gas phase and in polar solvents, as a function of central torsion angle.

torsion angle. The magnitude of these changes, however, is much smaller than those in the gas phase. In Figure 6, the partial charge in each ring moiety changes in a similar form to that in the gas phase. However, most notably, the partial charges in each ring do not appear to be significantly altered by torsion in comparison with the case of the gas phase.

In acetonitrile, the solute dipole moment changes from 20.4 to 22.0 D with increasing torsion angle, with a dipole moment of 21.20 D from partial charges (cf. 21.29 D from the ab initio wave function) at the optimized torsion angle. In aqueous solution, the solute dipole moment derived from partial charges is even greater, 27.53 D for the optimized structure (cf. 27.68 D by the ab initio wave function). The dipole moment in water shows even less change with increasing torsion angle (Figure 4). Figure 6 indicates that the partial charges in each ring do not change much with twisting the torsion angle. The central C−N bond, however, is shortened by only about 0.01 Å, by changing the torsion angle from 0° to the optimum value. The small effects of the shortening of the central bond and the slight variation in polarization in the solute molecule tend to cancel, and thus the solute dipole moment does not display a significant change.

Two aspects of these results for the dipole moment are particularly remarkable. First, the dipole moment enhancement in the strongly polar solvents is very large (∼7 D in acetonitrile, ∼14 D in water for the planar geometry). Comparable increases reported previously,[13,15] based on semiempirical calculations, are evidently not an artifact of the approximate quantum chemistry. In particular, the quite simplified π-electron treatment used in earlier simulations[13] appears justified in its treatment of this feature ($\mu_{gas} = 16$ D, $\mu_{CH_3CN} = 25$ D at $\chi = 53°$). Second, the polarization is sufficiently strong that the torsional dependence of the charge separation that is evident in the gas phase is much weaker in polar solvent. This polarization effect will be seen below to strongly effect the torsion angle dependence of the electronic energy and solvation free energy, including the correlation energy.

The relationship between the solute dipole moment and the solvation free energy is discussed next in section C.

C. Energy Profile. Figure 7 shows the comparison between energy profiles of the betaine solute with respect to the torsion angle in the gas and solution phases, including consideration of solvation and electron correlation effects. It can be seen that

the torsion angle at each minimum in the energy profile is shifted toward a larger value with increasing solvent polarity. The minima occur at about 30° in the gas phase, 46° in acetonitrile. and 47° in aqueous solution. Even more striking is the variation in the barrier to reaching the fully twisted state. These results show that the free energy surface for solute geometry change depends dramatically on solvent effects. We will discuss details for each case below.

1. Gas Phase. Referring again to the gas-phase data in Figure 2, the magnitude of the electron correlation energy decreases with increasing torsion angle in the gas phase. In the perpendicular conformation, the correlation energy is about 9 kcal mol^{-1} less negative than for the coplanar conformation. This indicates that, along with enlargement of the torsion angle, charge separation is improved (see Figure 6) and a decrease in the π-electron interaction between rings reduces electron correlation effects between the two rings.

It should be noted that this behavior is very different from that observed for an apparently similar solute, biphenyl. Biphenyl is composed of two benzene rings, whereas the present system has the pyridinium and phenoxide rings, with the pyridinium ring acting as an electron acceptor and the phenoxide an electron donor. Therefore, it seems that these remarkable properties are particular to the betaine. To confirm this, the same calculations as those described above were performed for the biphenyl case (for both the coplanar and the perpendicular conformation). The energy difference between the perpendicular and coplanar conformations, about -0.37 kcal mol^{-1}, was estimated with inclusion of the electron correlation effect. Note that this result is in good agreement with the experimental result,[44] 0 kcal mol^{-1}, and previously reported calculated results,[28] -0.25 kcal mol^{-1}. Compared with the betaine molecule, the energy difference is very small.

2. In Acetonitrile. In Figure 8a, the variation of total free energy is shown, including the excess chemical potential, solute energy, and electron correlation energy of the solute molecule in acetonitrile.

As the torsion angle increases, the total free energy decreases with a minimum at 46°, at which the solute molecule attains the optimum structure. This result is in good accord with previous studies of the related molecule betaine-30, 48°[17] and 53°.[13] In the range $\chi = 0$ to 46°, the solute energy and the excess chemical potential from solvation both decrease relative to the values in the coplanar structure. As $\chi \rightarrow 90°$, the excess chemical potential decreases somewhat further, corresponding to increasing solute dipole moment, shown in Figure 4. In addition, steric hindrance between hydrogen atoms [e.g., between H(10) and H(19), see Figure 1] is further somewhat reduced and solvation through weak "hydrogen bonding" between the H site in the solute and the nitrogen atom in CH_3CN is enhanced. The solute energy becomes larger than at the minimum as in the gas phase (see Figure 2), due to loss of inter-ring conjugation.

The electronic energy difference between the minimum structure and that with $\chi = 90°$ shows only a slight increase (about 1 kcal mol^{-1}) in polar solvents when electron correlation is not treated. However, with inclusion of the correlation energy, the energy difference is enhanced by more than 2 kcal mol^{-1}, and the minimum appears clearly. These results indicate that for the betaine solute in acetonitrile, the solute electron correlation energy plays an important role. However, it is notable that the change in electron correlation energy is only about half as large as in the gas phase. The electronic polarization of the solute reduces the dependence of the correlation energy on the torsion angle.

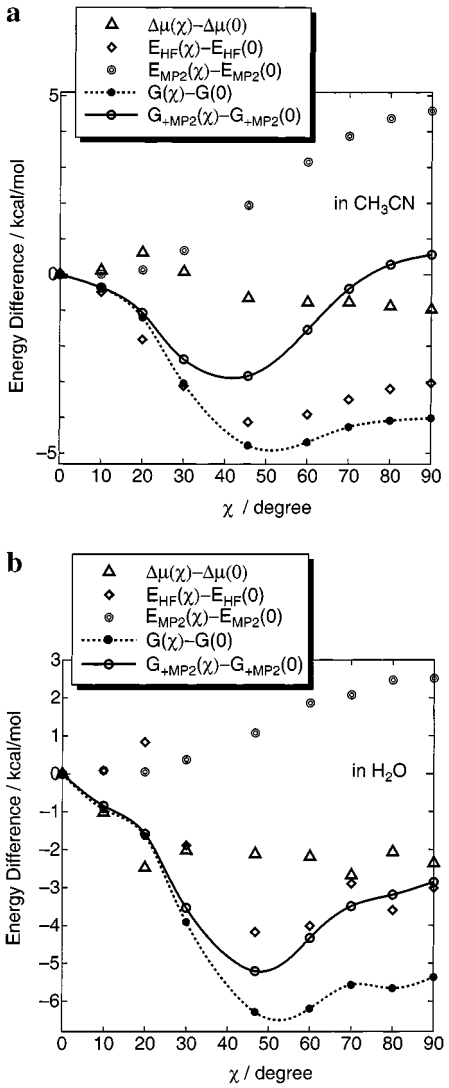

Figure 8. Torsional energy profiles, relative to planar, in polar solvents. (a) Acetonitrile and (b) water. The excess chemical potential $\Delta\mu$, the solute energ E_{HF}, and the solute electronic correlation energy E_{MP2}, are shown. The total free energies G and G_{+MP2} are without or with correlation energy, respectively.

3. In Water. In Figure 8b, the total free energy surface and its constituents in aqueous solution are shown. Compared with the energy profile in acetonitirile, the optimal point is shifted toward a slightly larger value, 47°. Here, it should be noted that there is a discrepancy regarding the solute geometry in water between this and a previous report from Bartkowiak and Lipiński.[16] These authors reported that the optimized torsion angle for betaine dye systems including the one used in the present study, in aqueous solution is 90° for every case. They also reported, however, that for betaine-30, which is similar to the present system, the oscillator strength showed a maximum at about 40°, and becomes almost zero in the reported optimal perpendicular conformation. The betaine dyes are distinguished by their strong absorption of light (and the solvatochromic shift exhibited). The oscillator strength reported in ref 16 is therefore inconsistent with a perpendicular configuration. The origin of this problem is presumably the fact that these earlier calculations used a continuum SCRF solvent description, although they carried out ab initio calculations. Hydrogen bonding between the solute and solvent is important in aqueous solution and such effects are not included in the SCRF method.

In contrast to acetonitrile, for water the excess chemical potential becomes more negative with increase in the central torsion angle at small angles ($\lesssim 30°$). This means that, as the geometry changes, the solvation process is improved through strong hydrogen bonding between the solute and solvent molecules. Correspondingly, the solute energy actually increases slightly compared to that in the coplanar form, since an additional electronic polarization is induced by the interactions with the solvent. At angles $\chi > 30°$, the solute energy becomes lower and exhibits a minimum at the optimized torsion angle. The excess chemical potential continues to decrease gradually even after the optimal point, as in acetonitrile. However, the degree of this decrease is very small. This is in accord with the variation of the solute dipole moment discussed above. In water, the additional solvent polarity induces the full charge separation at a smaller angle.

The energy profile changes by about 1 kcal mol^{-1} between the optimized angle and 90° without inclusion of electron correlation. The difference, however, becomes larger with the solute electron correlation energy included, where it is enhanced to about 2 kcal mol^{-1}. Although these results are qualitatively similar to those in acetonitrile, the variation in correlation energy is reduced in water. Further, the overall variation in correlation energy with angle is only about 25% of that in the gas phase.

D. Conclusion

The RISM-SCF method has been employed to study the simplest betaine dye (pyridinium-*N*-phenoxide) in the polar solvents CH_3CN and H_2O. The solute geometry, dipole moment, free energy profile, and the solute electron correlation energy in the solvents was investigated. The same properties were calculated in the gas phase for comparison purposes.

The geometry of the solute molecule in the gas phase has a twisted form. The optimum torsion angle between the pyridinium and phenoxide rings was found to be about 40° at the RHF level. CASSCF level calculations carried out for the ground-state yield an optimum geometry in good agreement with the RHF result.

In polar solvents, the results indicate that the torsion angle is enlarged to 45.56° in acetonitrile and 46.79° in aqueous solution at the RISM-SCF level. A key observation is that the solute dipole does *not* change remarkably in solution as a function of the torsion angle, in comparison with that in the gas phase. However, direct transfer of the optimum gas phase structure to solution does lead to a very large increase in dipole moment. The dipole moment increase from about 15 D at the optimal gas phase structure to about 21 D in acetonitrile and to about 28 D in water is consistent with earlier semiempirical values.[13,16] It was shown that the dipole moment changes are qualitatively consistent with the behavior of the excess chemical potential.

In the estimation of the total free energy, the electron correlation energy of the solute molecule was taken into account. The potential energy surface with respect to the torsion angle was computed, and it was shown that the magnitude of the electron correlation energy was reduced with increasing torsion angle. This is consistent with our results that both the solute dipole moment and the central C(12)−N(6) distance increase monotonically with increasing χ. It was also shown that this correlation energy effect was particular to the charge-separated betaine solute, and it is not a feature of the otherwise apparently similar biphenyl. Consequently, the total free energy profile has a very distinct minimum at the optimum torsion angle, and the energy difference between this minimum and 90° is enhanced by correlation energy. The effect of the solute correlation energy plays a critical role in the total free energy curve in the gas phase, and a distinct but a much smaller role in solution.

The magnitude of change in correlation energy with increasing torsion angle decreases with increasing solvent polarity (gas → acetonitrile → water). While the charge separation between the two main rings does not differ significantly in the two polar solvents, distribution of charge does. This is reflected in the difference in behavior of the correlation energies with torsion angle, which vary by a factor of 4 less in water than in the gas phase. The correlation energy effects and solvation free energy variation with torsion angle tend to cancel. Hence, one finds that the HF energy *for the polarized solute* is an increasingly accurate description of the total free energy with increasingly polar solvents.

Of particular note is the relevance of the results to partial charge models of solutes. For the betaines, we find that the solvent-induced polarization is a key factor. However, the variation in charges with torsional angle is a relatively small effect in polar solution, compared to the gas phase. Correspondingly, charges based on gas-phase calculations would not yield a reliable model for either the magnitudes or geometric dependence.

For the present system, solvatochromic, geometric, and dynamic behavior following excitation in solution are of interest.[45] A study along the present lines for the S_1 excited state will give more detailed information. This research is now in progress.

Acknowledgment. We thank to Dr. R. Westacott for helpful comments on the manuscript. The authors are grateful for support of this research by a grant from the National Science Foundation.

References and Notes

(1) Reichardt, C. *Solvents and Solvent Effects in Organic Chemistry*, 2nd ed; VCH: Weinheim, 1988.
(2) Suppan, P.; Ghoneim, N. *Solvatochromism*; Cambridge: Royal Society of Chemistry, 1997.
(3) Reichardt, C. *Angew. Chem.* **1979**, *91*, 119; *Angew. Chem., Int. Ed. Engl*. **1979**, *18*, 98; *Chem. Rev*. **1994**, *94*, 2319.
(4) Levinger, N. E.; Johnson, A. E.; Walker, G. C.; Barbara, P. F. *Chem. Phys. Lett.* **1991**, *196*, 159.
(5) Walker, G. C.; Åkesson, E.; Johnson, A. E.; Levinger, N. E.; Barbara, P. F. *J. Phys. Chem*. **1992**, *96*, 3728.
(6) Kjaer, A. M.; Ulstrup, J. *J. Am. Chem. Soc*. **1987**, *109*, 1934.
(7) Zong, Y.; McHale, J. L. *J. Chem. Phys*. **1997**, *106*, 4963.
(8) Bixon, M.; Jortner, J. *J. Chem. Phys*. **1993**, *176*, 467.
(9) Zhu, J.; Rasaiah, J. C. *J. Chem. Phys.* **1994**, *101*, 9966.
(10) Gayathri, N.; Bagchi, B. *J. Chem. Phys.* **1996**, *93*, 1652.
(11) Åkesson, E.; Walker, G. C.; Barbara, P. F. *J. Chem. Phys*. **1991**, *95*, 4188.
(12) Lobaugh, J.; Rossky, P. J. *J. Phys. Chem. A.* **1999**, *103*, 9432.
(13) Lobaugh, J.; Rossky, P. J. *J. Phys. Chem. A.* **2000**, *104*, 899.
(14) Ishida, T.; Hirata, F.; Sato, H.; Kato, S. *J. Phys. Chem. B* **1998**, *102*, 2045.
(15) De Alencastro, R. B.; Da Motta Neto, J. D.; Zerner, M. C. *Int. J. Quantum Chem. Quantum Chem. Symp*. **1994**, *28*, 361; *Chem. Abstr*. **1995**, *122*, 83696t.
(16) Bartkowiak, W.; Lipiński, J. *J. Phys. Chem. A* **1998**, *102*, 5236.
(17) Mente, S. R.; Maroncelli, M. *J. Phys. Chem. B* **1999**, *103*, 7704.
(18) Allmann, R. *Z. Kristallogr*. **1969**, *128*, 115.
(19) Perng, B.-C.; Newton, M. D.; Raineri, F. O.; Friedman, H. L. *J. Chem. Phys*. **1996**, *104*, 7153.
(20) Perng, B.-C.; Newton, M. D.; Raineri, F. O.; Friedman, H. L. *J. Chem. Phys*. **1996**, *104*, 7177.
(21) Ten-no, S.; Hirata, F.; Kato, S. *Chem. Phys. Lett*. **1993**, *214*, 391.
(22) Ten-no, S.; Hirata, F.; Kato, S. *J. Chem. Phys*. **1994**, *100*, 7443.
(23) Sato, H.; Hirata, F.; Kato, S. *J. Chem. Phys.* **1996**, *105*, 1546.
(24) Naka, K.; Sato, H.; Morita, A.; Hirata, F.; Kato, S. *Theor. Chem. Acc.* **1999**, *102*, 165.
(25) Tsuzuki, S.; Tanabe, K. *J. Phys. Chem.* **1991**, *95*, 139.
(26) Rubio, M.; Merchán, M.; Orti, E. *Theor. Chim. Acta* **1995**, *91*, 17.

(27) Rubio, M.; Merchán, M.; Ortí, E.; Roos, B. O. *Chem. Phys. Lett*. **1995**, *234*, 373.
(28) Tsuzuki, S.; Uchimaru, T.; Matsumura, K.; Mikami, M.; Tanabe, K. *J. Chem. Phys*. **1999**, *110*, 2858.
(29) Ould-Moussa, L.; Poizat, O.; Castellá-Ventura, M.; Buntinx, G.; Kassab, E. *J. Phys. Chem*. **1996**, *100*, 2072.
(30) Karpfen, A.; Choi, C. H.; Kertesz, M. *J. Phys. Chem. A* **1997**, *101*, 7426.
(31) Castellá-Ventura, M.; Kassab, E. *J. Raman. Spectrosc*. **1998**, *29*, 511.
(32) Rao, J. L.; Bhanuprakash, K. *J. Mol. Struct. (THEOCHEM)* **1999**, *458*, 269.
(33) Fabian, J.; Rosquete, G. A.; Montero-Cabrera, L. A. *J. Mol. Struct. (THEOCHEM)* **1999**, *469*, 163.
(34) Hirata, F.; Rossky, P. J. *Chem. Phys. Lett*. **1981**, *83*, 329.
(35) Hirata, F.; Pettitt, B. M.; Rossky, P. J. *J. Chem. Phys*. **1982**, *77*, 509.
(36) Hirata, F.; Rossky, P. J.; Pettitt, B. M. *J. Chem. Phys*. **1983**, *78*, 4133.
(37) Ishida, T.; Hirata, F.; Kato, S. *J. Chem. Phys*. **1999**, *110*, 3938.
(38) T. H. Dunning, J.; Hey, P. J. *Modern Electronic Structure Theory*; Plenum: New York, 1977.
(39) Sato, H.; Kovalenko, A.; Hirata, F. *J. Chem. Phys*. **2000**, *112*, 9463.
(40) Jorgensen, W. L.; Briggs, J. M.; Contreras, M. L. *J. Phys. Chem*. **1990**, *94*, 1683.
(41) Jorgensen, W. L.; Severance, D. L. *J. Am. Chem. Soc*. **1990**, *112*, 4768.
(42) Jorgensen, W. L.; Briggs, J. M. *Mol. Phys*. **1988**, *63*, 547.
(43) Brendsen, H. J. C.; Postma, J. P. M.; von Gustern, W. F.; Hermas, J. *Intermolecular Forces*; Reidel: Dordrecht, 1981.
(44) Carreira, L. A.; Towns, T. G. *J. Mol. Struct.* **1977**, *41*, 1.
(45) González, D.; Neilands, O.; Rezende, M. C. *J. Chem. Soc., Perkin Trans. 2* **1999**, *4*, 713.